Pilot-Aided Multicarrier Channel Estimation via MMSE Linear Phase-Shifted Polynomial Interpolation

Kun-Chien Hung and David W. Lin, *Senior Member, IEEE*

***Abstract*—Current wireless multicarrier systems commonly adopt pilot-aided channel estimation, for which a simplest and least restrictive technique is polynomial interpolation in the frequency domain. For channels with large delay spreads, however, the performance of low-order polynomial interpolation suffers from modeling error. The problem may be remedied by adding a linear phase shift to the interpolator, or equivalently, a "window shift" in the time domain. We derive a method to estimate the optimal window shift, in the minimum mean-square error (MMSE) sense, for polynomial-interpolative channel estimation of arbitrary order. As a practical application, we show how to apply the resultant technique to Mobile WiMAX downlink channel estimation. In addition, we propose a method to automatically select the interpolation order based on some estimated MSE.**

***Index Terms*—Channel estimation, delay estimation, orthogonal frequency-division multiple access (OFDMA), orthogonal frequency-division multiplexing (OFDM), polynomial interpolation.**

I. Introduction

COHERENT multicarrier transmission requires channel state information. Hence wireless multicarrier systems today commonly transmit pilots to facilitate channel estimation. Pilots are subcarriers that carry known signals. They may be dispersed in frequency and/or in time. A typical channel estimator starts by estimating the channel responses at the pilot subcarriers. Then it "fleshes out" the estimate for other subcarriers in some way. Three primary types of pilot-aided channel estimation methods are model-based, Wiener filtering, and channel-independent interpolation.

Model-based methods attempt to identify the the multipath delays. The channel is then estimated via projection onto the so-called "delay subspace." Such methods can achieve good performance with few pilots, but two main concerns are the complexity and the robustness of delay subspace estimation [1]–[4], especially when the multipath delays are not sample-spaced.

Wiener, or linear minimum mean-square error (LMMSE), filtering, has been considered widely [5]–[9]. However, it requires the channel correlation function, which raises problems not only in the complexity of correlation estimation but also in the impact of estimation accuracy on channel estimation performance. A suboptimal solution is to use a predefined shape for the correlation function, such as that associated with a uniform [9] or an exponential power-delay profile (PDP) [5], [10]. Nevertheless, one still needs to estimate the parameters of the PDP.

Channel-independent interpolation methods seek to reconstruct the channel responses at data subcarriers by channel-independent interpolation of the channel estimates at pilot subcarriers. The simplest of them is low-order polynomial interpolation in the frequency domain [11]. The maximum-likelihood (ML) interpolator [7] is a more sophisticated member of them, but it requires that the number of pilots be no smaller than the length of the channel impulse response.

In short, an ideal channel estimator should require as few pilots as possible, have good estimation perfomance and low computational complexity, and be robust to variations in channel and operating conditions. Existing techniques are open to improvement in one or another of these aspects. In this work, we consider the lowest-complexity approach, namely, polynomial interpolation, which also appears to be the most robust and most broadly applicable of all approaches. We seek to enhance its performance without significant increase in complexity. We assume that the synchronization of carrier frequency and multicarrier symbol timing is done prior to channel estimation. Further, we assume that the carrier frequency synchronization is rather accurate while the symbol timing synchronization may be less so. These are reasonable assumptions, for example, in downlink (DL) Mobile WiMAX transmission [12], [13].

To begin, we first note that, of all polynomial interpolation schemes, a simplest and most commonly considered is linear interpolation. For this scheme, it has been found that the channel estimation performance may suffer greatly not only in poor symbol synchronization [14] but also when the channel has a large delay spread [15]. One way to alleviate the problem is to use a higher interpolation order [11]. The reason why different interpolation orders may give different performance

Manuscript received May 4, 2009; revised September 28, 2009, January 27, 2010, and April 16, 2010; accepted May 25, 2010. The associate editor coordinating the review of this paper and approving it for publication was X. Gao.

K.-C. Hung was with the Department of Electronics Engineering and Institute of Electronics, National Chiao Tung University, Hsinchu, Taiwan 30010. He is now with MediaTek Inc., 1 Dusing Rd. 1, Hsinchu Science Park, Hsinchu, Taiwan 30078 (e-mail: hkc.ee90g@nctu.edu.tw).

D. W. Lin is with the Department of Electronics Engineering and Institute of Electronics, National Chiao Tung University, Hsinchu, Taiwan 30010 (e-mail: dwlin@mail.nctu.edu.tw).

This work was supported in part by the National Science Council of the Republic of China under Grant NSC 97-2219-E-009-009. Part of this work was presented at IEEE Globecom 2008, New Orleans, LA, USA.

Digital Object Identifier 10.1109/TWC.2010.061010.090467

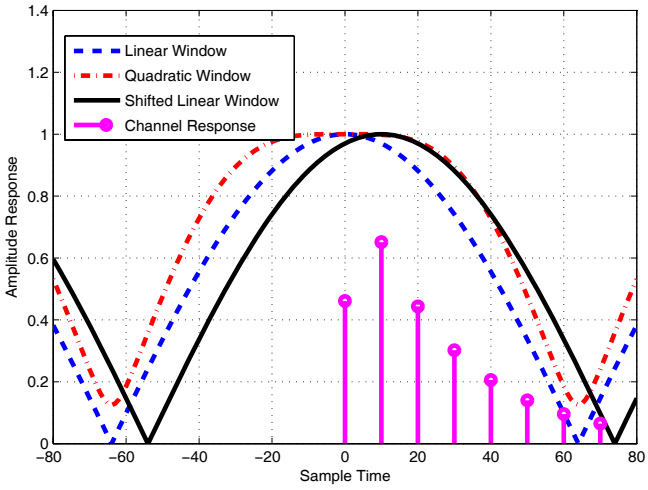

Fig. 1. Comparison of different ways of interpolation in terms of the equivalent time-windowing effects.

can be interpreted via some well-known results in signal processing theory, which not only provide a useful perspective for understanding and analysis of the phenomenon but also hint at improved interpolator design. Specifically, polynomial interpolation amounts to a sort of linear filtering [16]. Since convolution in the frequency domain corresponds to multiplication in the time domain, different orders of interpolation of the frequency response correspond to different kinds of windowing on the channel impulse response. Fig. 1 is a conceptual illustration [17]. Linear interpolation (dashed line) corresponds to a smaller window size than quadratic interpolation (dash-dot line) and hence results in greater distortion of the channel response. However, if one can shift the window corresponding to linear interpolation by some amount to better capture the time range of significant channel response samples (solid line), then one may improve its performance. The same also applies to higher-order interpolation.

Now the question is: how to determine the optimal window shift for a given interpolation order? As shifting a signal in time amounts to modulating its frequency spectrum with a single complex exponential, Hsieh and Wei [11] adopt the single frequency estimators of Kay [18] to find the desired offset. Unfortunately, for channel estimation these estimators are not optimal in the MSE sense [15]. We will derive the optimal window shift that attains MMSE in channel estimation for arbitrary polynomial order. Another interesting question is how the required window shifting (in time) or the equivalent linear phase rotation (in frequency) may be realized. Earlier studies [11], [15] have employed straightforward linear phase rotation in the frequency domain. We will see that, when the amount of shift is an integer multiple of the sample period, a much simpler alternative exists which involves mere circular shifting of signal samples.

It is instinctively expected that the MMSE in channel estimation should depend on the amount of channel noise. In fact, later analysis will show that, in high channel noise, higher-order interpolation may be affected so more adversely than lower-order interpolation as to yield worse channel estimates. Therefore, it would be desirable if the interpolation order can be selected adaptively according to the channel condition to attain the best possible channel estimation performance. We will also address this issue.

In summary, the contributions of this paper are: 1) a low-complexity channel estimation technique based on linear phase-shifted polynomial interpolation, 2) specialization of the technique to DL Mobile WiMAX transmission, and 3) a technique for adaptive selection of the polynomial interpolation order. In what follows, Section II considers the estimation of MMSE window shift under given polynomial order. Section III evaluates its performance in noisy channel under comb-type pilots. Section IV adapts the technique to suit the Mobile WiMAX DL signal, which has an interesting pilot structure that necessitates some additional design work. We also investigate the adaptive selection of interpolation order in this context. Finally, Section V concludes the paper.

II. MMSE Window Shifting

Consider a sampled equivalent lowpass channel impulse response

$$h(n) = \sum_{l=0}^{L-1} \alpha_l \delta(n-l) \tag{1}$$

where n and l are integers in units of the sampling period T_s, α_l is the complex gain of path l, and $(L-1)T_s$ is the maximum path delay. The corresponding frequency response is given by

$$H(f) = \sum_{l=0}^{L-1} \alpha_l e^{-j2\pi lf/N} \tag{2}$$

where N is the size of discrete Fourier transform (DFT) used in multicarrier transformation and the division by N in the exponent term normlizes the subcarrier spacing in the multicarrier system to unity as well as normalizes the period of $H(f)$ in f to N.

Consider comb-type pilot allocation and let the mth pilot subcarrier be located at frequency $p_0 + mF$ where p_0 is the lowest pilot subcarrier frequency and F is the spacing of pilot subcarriers. (The treatment can be readily extended to noncomb-type pilots, but the equations become somewhat cumbersome.) Let $\hat{H}(p)$ denote the channel estimate at any pilot subcarrier p, however it may be obtained. Then conventional polynomial interpolation between two pilot locations $p = p_0 + mF$ and $p + F = p_0 + (m+1)F$ can be written as

$$\hat{H}(p+n) = \sum_{k=0}^{K} c_{nk}\, \hat{H}(p + x_{nk}) \tag{3}$$

where $0 < n < F$, K is the interpolation order, x_{nk} is an integer multiple of F that defines the kth pilot location used in interpolation, and c_{nk} is the corresponding interpolation coefficient. Usually, x_{nk} should be as small in magnitude as possible so that the interpolating pilots $p + x_{nk}$ are as close to the frequency $p + n$ as possible, but this point does not matter for now. The coefficients that yield error-free interpolation of any polynomial function of order K or below are known [19].

They are real and can be written in the Vandermonde form as

$$\begin{aligned}\mathbf{c}'_{nK} &\triangleq [c_{n0} \quad c_{n1} \quad \cdots \quad c_{nK}] \\ &= \underbrace{[1 \quad n \quad \cdots \quad n^K]}_{\triangleq \mathbf{v}'_{nK}} \underbrace{\begin{bmatrix} 1 & x_{n0} & \cdots & x_{n0}^K \\ 1 & x_{n1} & \cdots & x_{n1}^K \\ \vdots & \vdots & \ddots & \vdots \\ 1 & x_{nK} & \cdots & x_{nK}^K \end{bmatrix}^{-1}}_{\triangleq \mathbf{X}_{nK}}, \quad (4)\end{aligned}$$

where $'$ denotes transpose, or in the Lagrange form as [20, §25.2.2]

$$c_{nk} = \prod_{m=0, m\neq k}^{K} \frac{n - x_{nm}}{x_{nk} - x_{nm}}, \quad 0 \le k \le K. \quad (5)$$

Now consider phase-rotated interpolation corresponding to a time window delay of τ samples, where the optimal value of τ is to be found. (In principle, τ needs not be an integer.) To see how it affects (3), consider an arbitrary frequency-domain filter with input $a(f)$, output $b(f)$, and impulse response $c(f)$. A τ-sample delay of the time window corresponding to $c(f)$ amounts to a linear phase rotation of the frequency-domain impulse response to $e^{-j2\pi\tau f/N}c(f)$. That is, the input-output relation is changed from $b(f) = \sum_{f'} c(f-f')a(f')$ to $b(f) = \sum_{f'} e^{-j2\pi\tau(f-f')/N}c(f-f')a(f')$. Identifying f with $p+n$ and f' with $p + x_{nk}$, we get, for (3),

$$\begin{aligned}&\hat{H}(p+n) \\ &= \sum_{k=0}^{K} e^{-j2\pi\tau(n-x_{nk})/N} c_{nk} \hat{H}(p+x_{nk}) \\ &= e^{-j2\pi\tau(p+n)/N} \sum_{k=0}^{K} c_{nk} \left[e^{j2\pi\tau(p+x_{nk})/N} \hat{H}(p+x_{nk}) \right]. \quad (6)\end{aligned}$$

By substituting $p + x_{nk}$ with f in the last bracketed term, we see that this term indicates a phase rotation of the pilot subcarrier channel estimates by an amount corresponding to a τ-sample time advance. The right-hand side (RHS) of (6) can thus be interpreted as indicating a four-step procedure for channel estimation under given τ as follows: 1) obtain the pilot subcarrier channel estimates $\hat{H}(p + x_{nk})$ by some method, 2) phase-rotate the pilot subcarrier channel estimates by an amount corresponding to a τ-sample time advance (as indicated by the bracketed term in (6)), 3) perform conventional polynomial interpolation to obtain the data subcarrier channel estimates (as indicated by the last summation in (6)), and 4) phase-derotate the channel estimates from the last step by an amount corresponding to a τ-sample time delay (as indicated by the premultiplication by $e^{-j2\pi\tau(p+n)/N}$ in (6)).

As mentioned previously, when τ is an integer, a simple time-domain equivalent exists for steps 2 and 4. Specifically, for an integer τ, if we shift the received signal circularly by $-\tau$ samples before taking its DFT, the channel response is effectively advanced by τ samples. Working with the circularly shifted signal, the phase rotation and derotation can be saved. More details will be given in Section IV when we consider Mobile WiMAX DL transmission. But for convenience, the theoretical derivation below employs the formulation based on phase rotation.

Now we turn to the key issue of determining τ. For this we first find how the channel estimation MSE depends on τ under arbitrary polynomial interpolation order. Then we derive a suboptimal solution for τ and consider its computational complexity.

A. MSE as Function of Window Shift

Consider advancing the channel impulse response by τ samples. The resultant frequency response is given by

$$H_\tau(f) \triangleq e^{j2\pi\tau f/N} H(f) = \sum_{l=0}^{L-1} \alpha_l e^{-j2\pi(l-\tau)f/N}. \quad (7)$$

Laying together the first RHS in (7) and the bracketed term in (6), we see that the bracketed term may be viewed as an estimate of $H_\tau(p + x_{nk})$. More generally, let

$$\hat{H}_\tau(f) = e^{j2\pi\tau f/N} \hat{H}(f). \quad (8)$$

Then (6) can be rewritten as

$$\hat{H}_\tau(p+n) = \sum_{k=0}^{K} c_{nk} \hat{H}_\tau(p + x_{nk}). \quad (9)$$

The MSE in $\hat{H}_\tau(p+n)$ (as estimate of $H_\tau(p+n)$) is the same as that in $\hat{H}(p+n)$ (as estimate of $H(p+n)$), for the two estimates are related by mere phase rotation. Hence we derive the former. To concentrate on the modeling error of interpolation, we ignore the effect of channel noise for the moment. That is, we assume temporarily that $\hat{H}_\tau(p+x_{nk}) = H_\tau(p + x_{nk})$. In fact, mathematics below shows that white channel noise does not affect the optimal window shift.

The Kth-order Taylor series expansion of $H_\tau(p+n)$ about a subcarrier p is given by

$$H_\tau(p+n) = \sum_{k=0}^{K} \frac{H_\tau^{(k)}(p) n^k}{k!} + \rho_K(p+n) \quad (10)$$

where $H_\tau^{(k)}(p)$ denotes the kth derivative of $H_\tau(p)$ and $\rho_K(p+n)$ is the remainder term. By the integral form of the remainder term [20, §25.2.25],

$$\begin{aligned}\rho_K(p+n) &= \int_0^n \frac{H_\tau^{(K+1)}(p+u)}{K!} (n-u)^K du \\ &= \sum_{l=0}^{L-1} \alpha_l \left[\frac{-j2\pi(l-\tau)}{N} \right]^{K+1} e^{-j2\pi(l-\tau)p/N} \\ &\quad \cdot \int_0^n \frac{e^{-j2\pi(l-\tau)u/N}}{K!} (n-u)^K du. \quad (11)\end{aligned}$$

From (9) and (4), the interpolation error for $H_\tau(p+n)$ is given by

$$\begin{aligned}&H_\tau(p+n) - \hat{H}_\tau(p+n) \\ &= H_\tau(p+n) - \mathbf{v}'_{nK} \mathbf{X}_{nK}^{-1} \cdot \mathrm{vec}\left[\hat{H}_\tau(p+x_{n0}), \right. \\ &\quad \left. \hat{H}_\tau(p+x_{n1}), \cdots, \hat{H}_\tau(p+x_{nK}) \right] \quad (12)\end{aligned}$$

where vec$[\cdot]$ denotes a vector of the items given in the brackets. Since no error arises in interpolating a polynomial function of

order K or below, all errors in (12) are from the remainder terms $\rho_K(p+n)$ and $\rho_K(p+x_{nk})$, $0 \le k \le K$. Hence

$$\begin{aligned} H_\tau(p+n) - \hat{H}_\tau(p+n) \\ = \quad \rho_K(p+n) - \mathbf{v}'_{nK}\mathbf{X}_{nK}^{-1} \cdot \mathrm{vec}\left[\rho_K(p+x_{n0}),\right. \\ \left.\rho_K(p+x_{n1}), \cdots, \rho_K(p+x_{nK})\right]. \end{aligned} \tag{13}$$

From (11), if subcarriers p and $p+n$ are spaced closely compared to the coherence bandwidth such that $e^{-j2\pi(l-\tau)u/N} \approx 1$ for $0 \le u \le n$, then

$$\int_0^n \frac{e^{-j2\pi(l-\tau)u/N}}{K!}(n-u)^K du \approx \frac{n^{K+1}}{(K+1)!} \tag{14}$$

and thence

$$\begin{aligned} \rho_K(p+n) \approx \frac{n^{K+1}}{(K+1)!} \\ \cdot \sum_{l=0}^{L-1} \alpha_l \left[\frac{-j2\pi(l-\tau)}{N}\right]^{K+1} e^{-j2\pi(l-\tau)p/N}. \end{aligned} \tag{15}$$

In fact, (15) gives an approximation of $\rho_K(p+n)$ for any value of n, not limited to $0 < n < F$, although its accuracy should tend to diminish as the magnitude of n increases. Using it to approximate $\rho(p+x_{nk})$ $(0 \le k \le K)$ also and substituting the result into (13), we get

$$\begin{aligned} H_\tau(p+n) - \hat{H}_\tau(p+n) \\ \approx \quad \frac{1}{(K+1)!}\left[n^{K+1} - \mathbf{v}'_{nK}\mathbf{X}_{nK}^{-1}\mathbf{x}_{nK}\right]\xi_K(p,\tau) \end{aligned} \tag{16}$$

where

$$\mathbf{x}_{nK} = \left[x_{n0}^{K+1}, x_{n1}^{K+1}, \cdots, x_{nK}^{K+1}\right]', \tag{17}$$

$$\xi_K(p,\tau) = \sum_{l=0}^{L-1} \alpha_l \left[\frac{-j2\pi(l-\tau)}{N}\right]^{K+1} e^{-j2\pi(l-\tau)p/N}. \tag{18}$$

The interpolation MSE at a subcarrier located an offset n from a pilot can be estimated by taking the average of $|H_\tau(p+n) - \hat{H}_\tau(p+n)|^2$ over all pilots. It is shown in Appendix A that the bracketed term in (16) is equal to $\prod_{k=0}^{K}(n-x_{nk})$. As a result,

$$\begin{aligned} \langle\!\langle |H_\tau(p+n) - \hat{H}_\tau(p+n)|^2 \rangle\!\rangle \\ \approx \quad \left[\frac{\prod_{k=0}^{K}(n-x_{nk})}{(K+1)!}\right]^2 \langle\!\langle |\xi_K(p,\tau)|^2 \rangle\!\rangle \\ = \quad \left[\frac{\prod_{k=0}^{K}(n-x_{nk})}{(K+1)!}\right]^2 \\ \cdot \underbrace{\sum_{l=0}^{L-1} \frac{(2\pi)^{2K+2}}{N^{2K+2}}|\alpha_l|^2(l-\tau)^{2K+2}}_{\triangleq \sigma^2_{\xi_K}(\tau)} \end{aligned} \tag{19}$$

where $\langle\!\langle \cdot \rangle\!\rangle$ denotes averaging over all pilot subcarriers. The second equality in (19) indicates that the MSE is dominated by the channel paths with larger values of $|\alpha_l|^2(l-\tau)^{2K+2}$.

B. Estimation of Optimal Window Shift

From the above results, the channel estimation MSE can be minimized by minimizing $\sigma^2_{\xi_K}(\tau)$. By elementary calculus, the approximately optimal window shift τ can be obtained by solving

$$\begin{aligned} \frac{d\sigma^2_{\xi_K}(\tau)}{d\tau} &= -\frac{(2\pi)^{2K+2}(2K+2)}{N^{2K+2}} \sum_{l=0}^{L-1} |\alpha_l|^2 (l-\tau)^{2K+1} \\ &= 0. \end{aligned} \tag{20}$$

Unfortunately, this requires knowing the multipath gains and delays, which are most likely unknown until after channel estimation. To sidestep this dilemma, note that since

$$H_\tau^{(K+1)}(f) = \sum_{l=0}^{L-1} \alpha_l \left[\frac{-j2\pi(l-\tau)}{N}\right]^{K+1} e^{-j2\pi(l-\tau)f/N}, \tag{21}$$

by Parseval's theorem we get $\sigma^2_{\xi_K}(\tau) = \langle |H_\tau^{(K+1)}(f)|^2 \rangle$ where $\langle \cdot \rangle$ denotes averaging over all frequencies. Thus minimizing $\sigma^2_{\xi_K}(\tau)$ is equivalent to minimizing $\langle |H_\tau^{(K+1)}(f)|^2 \rangle$. While $H_\tau^{(K+1)}(f)$ is usually not available, either, it can be approximated, for example, by the $K+1$st forward difference given by

$$\begin{aligned} D_{K+1}H_\tau(f) \\ = \frac{1}{F^{K+1}} \sum_{k=0}^{K+1} (-1)^k \binom{K+1}{k} H_\tau(f + (K+1-k)F). \end{aligned} \tag{22}$$

The target of minimization can then be approximated by

$$\begin{aligned} \sigma^2_{\xi_K}(\tau) \approx \gamma \\ \triangleq \quad \frac{1}{F^{2K+2}} \cdot \left\langle\!\!\left\langle \left| \sum_{k=0}^{K+1} (-1)^k \right.\right.\right. \\ \left.\left.\left. \cdot \binom{K+1}{k} \hat{H}_\tau(p + (K+1-k)F) \right|^2 \right\rangle\!\!\right\rangle. \end{aligned} \tag{23}$$

Some algebraic manipulations result in

$$\gamma = \frac{1}{F^{2K+2}}\left[P_K R_0 + 2\gamma_K(\tau)\right] \tag{24}$$

where $P_K = 2^{K+1}(2K+1)!!/(K+1)!$, $R_k = \langle\!\langle \hat{H}(p+kF)\hat{H}^*(p) \rangle\!\rangle$, and

$$\gamma_K(\tau) = \Re\left\{\sum_{m=1}^{K+1} (-1)^m A_{Km} e^{-j2\pi m F\tau/N} R_m\right\} \tag{25}$$

with $\Re\{a\}$ denoting the real part of quantity a, $m!! = m(m-2)(m-4)\cdots x$ where $x = 2$ for even m and $x = 1$ for odd m, and

$$\begin{aligned} A_{Km} &= \sum_{k=m}^{K+1} \binom{K+1}{k}\binom{K+1}{k-m} \\ &= \frac{2^{K+1}(2K+1)!!(K+1)!}{(K+1-m)!(K+1+m)!}. \end{aligned} \tag{26}$$

Noting that only $\gamma_K(\tau)$ depends on τ, we may estimate the optimal window shift as

$$\hat{\tau} = \arg\min_\tau \gamma_K(\tau). \tag{27}$$

TABLE I
ORDER-OF-MAGNITUDE COMPARISON OF CHANNEL ESTIMATOR COMPLEXITY

Method	No. of Real Multiplications
Proposed	$2(K+1)(N+M+L/g)$
ML with radix-2 FFT	$2M\log_2 M + 2N\log_2 N$
ML with radix-4 FFT	$\frac{3M}{2}\log_2 M + \frac{3N}{2}\log_2 N$

For linear, quadratic and cubic interpolators, we have

$$\gamma_1(\tau) = \Re\left\{e^{-j2\theta}R_2 - 4e^{-j\theta}R_1\right\}, \quad (28)$$

$$\gamma_2(\tau) = \Re\left\{-e^{-j3\theta}R_3 + 6e^{-j2\theta}R_2 - 15e^{-j\theta}R_1\right\}, \quad (29)$$

$$\gamma_3(\tau) = \Re\left\{e^{-j4\theta}R_4 - 8e^{-j3\theta}R_3 + 28e^{-j2\theta}R_2 - 56e^{-j\theta}R_1\right\}, \quad (30)$$

where $\theta = 2\pi F\tau/N$. To compute $\hat{\tau}$ by (27), one way is to solve the equation $d\gamma_K(\tau)/d\tau = 0$ for τ that minimizes $\gamma_K(\tau)$. Unfortunately, algebraic solution exists only in the case of linear interpolation, for it is the only case where the equation has order under 5 [15]. Numerical solutions have to be resorted to in other cases. This being so, one might as well search over the range $[0, L-1]$ for the value of τ that minimizes $\gamma_K(\tau)$ rather than find it through solving $d\gamma_K(\tau)/d\tau = 0$. The density of searched points can be chosen according to the desired accuracy. By experience, we find that a suitable granularity is roughly 2 to 6 sample periods.

C. Computational Complexity

In summary, the proposed procedure to compute $\hat{\tau}$ for Kth-order interpolation is as follows: 1) Given pilot subcarrier channel response estimates $\hat{H}(p)$, calculate $R_k = \langle\!\langle \hat{H}(p+kF)\hat{H}^*(p)\rangle\!\rangle$, $1 \le k \le K+1$, and 2) search over the maximum range of path delays at a chosen granularity for the delay value τ that minimizes $\gamma_K(\tau)$ and let $\hat{\tau}$ be equal to it. Step 1 requires on the order of $4(K+1)M$ real multiplications (RMULTs) where M is the number of pilot subcarriers used to compute R_k. For step 2, the number of $\gamma_K(\tau)$ values to be computed is on the order of L/g where g is the search granularity. The $e^{j\theta}$ values corresponding to the searched delay values can be precomputed and stored. Then step 2 requires on the order of $2(K+1)L/g$ RMULTs. Thus the total computational complexity to obtain $\hat{\tau}$ is on the order of $(K+1)(4M+2L/g)$ RMULTs. In most system designs, it should be a fraction of the order of $2(K+1)(N-M)$ RMULTs for the interpolation proper.

It is of interest to compare the above with the complexity of ML interpolation. Given pilot subcarrier channel estimates $\hat{H}(p)$, ML interpolation can be achieved by taking the M-point inverse DFT (IDFT) of $\hat{H}(p)$, truncating the result to have maximum delay $L-1$, and taking the N-point DFT. Table I gives a comparison in number of RMULTs, assuming that radix-2 or radix-4 fast Fourier transform (FFT) can be used to carry out the IDFT and DFT in ML interpolation. Note that ML interpolation requires that $M > L-1$.

In current systems, the channel path delays usually do not vary significantly over several multicarrier symbols. Nor do the path gains vary violently over consecutive multicarrier symbols. These can be exploited to further reduce the complexity of the proposed technique. For example, after initialization, we may perform incremental search for the optimal $\hat{\tau}$ within a small range around the previous solution, rather than conducting a full search over the entire interval. Indeed, the optimal window shift may need be estimated only once every few symbols.

III. PERFORMANCE WITH COMB-TYPE PILOTS

Now consider the overall MSE of channel estimation by the proposed method in noisy channel for a system with comb-type pilots. Two reasons why we consider such a system are its relative ease of analysis and its ability to provide insights concerning the proposed method's performance.

To start, note that the estimation error arises from three sources, namely, 1) error from optimal interpolation (i.e., the minimum modeling error $H_\tau(p+n) - \hat{H}_\tau(p+n)$ attainable with optimal window shift), 2) use of the suboptimal window shift $\hat{\tau}$ of (27), and 3) the channel noise (which has been omitted thus far). The effect of source 2 (suboptimal estimation of window shift) defies a simple and general characterization because, as can be seen from the derivation from (19) to (27), it depends on the channel property in a complicated way. Fortunately, experience shows that when the pilots are reasonably dense, this error source contributes a minor amount in the total MSE. So we omit its effect in the analysis. Actually, we do not have an exact expression for source 1 (error of optimal interpolation), either, but only an approximation as given in (19). Thus the analysis is necessarily approximate. We assume that the channel noise is additive white Gaussian, i.e., AWGN, and independent of the modeling error.

For simplicity, let the pilot spacing F be an integer fraction of N. And let $\sigma^2_{eK}(n)$ denote the RHS of (19). Then from (19), the average MSE due to modeling error is approximately

$$\sigma^2_{eK} \triangleq \frac{1}{F-1}\sum_{n=1}^{F-1}\sigma^2_{eK}(n) = \underbrace{\frac{1}{F-1}\sum_{n=1}^{F-1}\left[\frac{\prod_{k=0}^{K}(n-x_{nk})}{(K+1)!}\right]^2}_{\triangleq q_K(F)}\cdot\sigma^2_{\xi K}(\tau^o) \quad (31)$$

where τ^o is the approximately optimal delay defined by (20). To be more specific of the values of $q_K(F)$, we need to define x_{nk} specifically. For this, consider letting x_{nk} lie in the range $-\lfloor K/2\rfloor F$ to $\lfloor (K+1)/2\rfloor F$ so that it is as small in magnitude as possible. And discard the nonpilot subcarriers that are too near a bandedge that there do not exist $K+1$ pilots in the above range for interpolation use. Then for linear, quadratic, and cubic interpolations we get

$$q_1(F) = \frac{1}{120}F(F+1)(F^2+1), \quad (32)$$

$$q_2(F) = \frac{1}{7560}F(F+1)(2F-1)(2F+1)(4F^2+5), \quad (33)$$

$$q_3(F) = \frac{1}{362880}F(F+1)\cdot(103F^6+103F^4+61F^2+21), \quad (34)$$

respectively. But $\sigma^2_{\xi K}(\tau^o)$ is channel-dependent and no general formulas can be given.

For the contribution of the AWGN, consider (3). Let the pilot signals have unity magnitude and let the pilot frequency responses $H(p)$ be estimated by the least-squares (LS) method, that is, by simply dividing the received signal value at each pilot subcarrier p by the pilot signal value there. Then the MSE in each $\hat{H}(p)$ is equal to the AWGN variance, which we denote by σ_η^2. Hence, the AWGN contribution in the channel estimation MSE at subcarrier $p+n$ is

$$\sigma_{wK}^2(n) \triangleq \sigma_\eta^2 \|\mathbf{c}_{nK}\|^2 = \sigma_\eta^2 \mathbf{v}'_{nK} \left(\mathbf{X}_{nK}\mathbf{X}'_{nK}\right)^{-1} \mathbf{v}_{nK} \quad (35)$$

(where $\mathbf{c}_{nK}$ is as defined in (4)) and the average over all data subcarriers is given by $\sigma_{wK}^2 = \sum_{n=1}^{F-1} \sigma_{wK}^2(n)/(F-1)$. In particular,

$$\sigma_{w1}^2 = \left(0.667 - \frac{0.333}{F}\right)\sigma_\eta^2, \quad (36)$$

$$\sigma_{w2}^2 = \left(0.8 - \frac{0.2}{F} + \frac{0.05}{F^2} + \frac{0.05}{F^3}\right)\sigma_\eta^2, \quad (37)$$

$$\sigma_{w3}^2 = \left(0.776 - \frac{0.224}{F} - \frac{0.058}{F^2} - \frac{0.058}{F^3} - \frac{0.013}{F^4} + \frac{0.013}{F^5}\right)\sigma_\eta^2. \quad (38)$$

The overall approximate channel estimation MSE is given by $\sigma_{eK}^2 + \sigma_{wK}^2$.

A. Numerical Examples

As an example, consider an orthogonal frequency-division multiplexing (OFDM) system with bandwidth = 10 MHz, DFT size $N = 1024$, cyclic prefix (CP) length = $N/8 = 128$, and pilot spacing $F = 4$. The window shift is obtained by search over all even-sample delays between 0 and 127. That is, the search granularity is 2 samples. We simulate the SUI-4 and SUI-5 PDPs [21], whose power profiles are $[0, -4, -8]$ and $[0, -5, -10]$ (in dB), respectively, and whose delay profiles are (approximately) $[0, 14, 36]$ and $[0, 45, 112]$ (in samples), respectively. The path coefficients are Rayleigh and block-static (constant over one symbol period). A total of 2000 simulation runs are used to obtain the MSE statistics for each signal-to-noise (SNR) value.

Fig. 2 shows histograms of the estimated window shifts for different interpolation orders over SUI-4 and SUI-5. Most shifts are quite a distance from zero, and they span a broad range within the limits of the delay spread, especially for the lower interpolation orders. Together with the MSE results below, this confirms the importance of proper window shifting on interpolation performance.

Fig. 3 illustrates the channel estimation performance of the proposed technique and compares it with conventional polynomial interpolation, LMMSE (4 taps), and ML (truncating to 128 samples between IDFT and DFT), where the MSE is normalized (NMSE) relative to the channel power gain. For LMMSE channel estimation, two conditions are simulated, one with filter coefficients calculated using the exact channel correlation functions (the "exact LMMSE" curves) and the other with them calculated using the channel correlation function corresponding to a uniform PDP of length equal to the CP (the "approx. LMMSE" curves). For SUI-4, the approximate analysis for phase-shifted interpolation yields

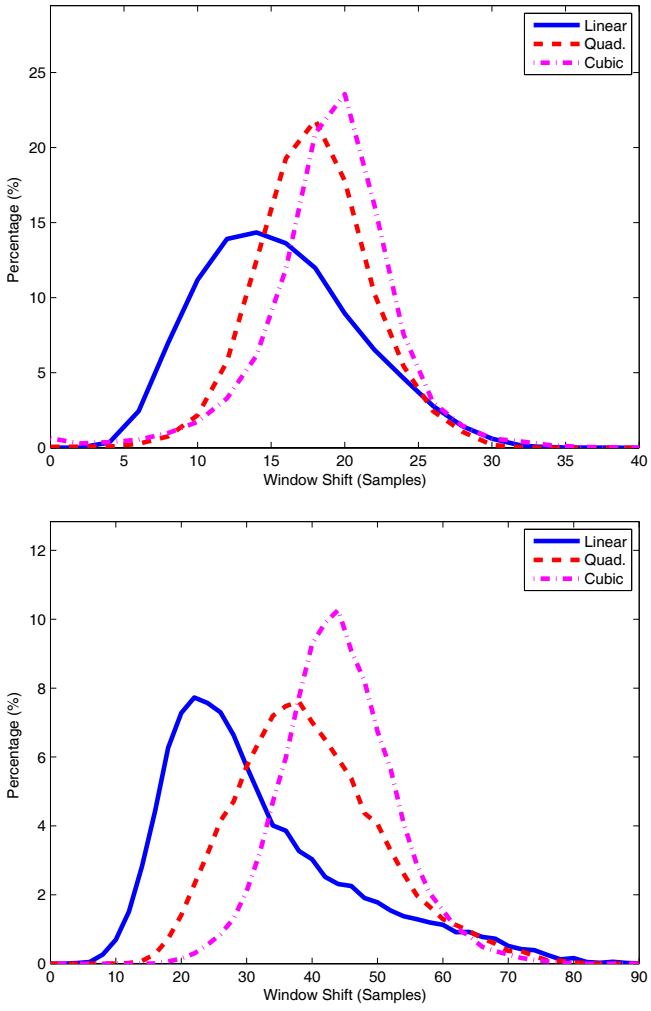

Fig. 2. Histograms of estimated window shifts for different orders of polynomial interpolations at 30 dB SNR. Top: over SUI-4; bottom: over SUI-5.

almost indistinguishable results from simulation. That for conventional polynomial interpolation is less accurate, as can be expected. At higher SNR values, conventional polynomial interpolation suffers significant loss from the MSE floors due to modeling errors, whereas phase-shifted interpolation can maintain a -1 slope in NMSE to much higher SNR values. For SUI-5, which has a greater delay spread than SUI-4, the approximate analysis tends to overestimate the MSE. And the error floors begin at lower SNR values than in SUI-4. However, the MSE floors of phase-shifted interpolation are much lower than that of conventional interpolation for all interpolation orders.

Not surprisingly, the best performer at any SNR is either the ML or the exact LMMSE. For ML channel estimation, since there are 256 pilots and we truncate to 128 samples between IDFT and DFT, its NMSE is uniformly better than the SNR by 3 dB. From Table I, phase-shifted polynomial interpolation takes on the order of 5376 (for $K = 1$) to 10752 (for $K = 3$) RMULTs, whereas ML interpolation on the order of 24576 (with radix-2 FFT) or 18432 (with radix-4 FFT) RMULTs. Regarding LMMSE channel estimation, exact LMMSE is not realizable. The approximate LMMSE

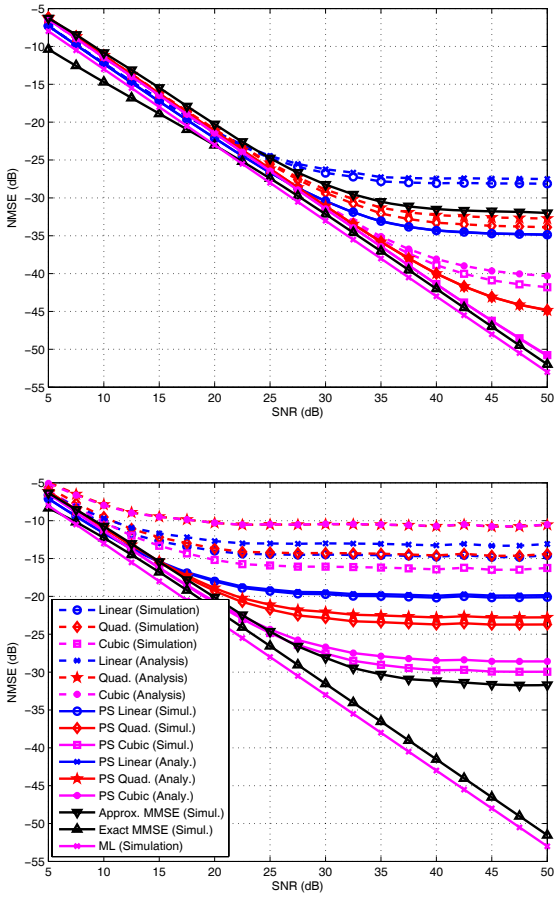

Fig. 3. NMSE of different channel estimation methods, where "PS" stands for "phase-shifted." Top: under SUI-4 PDP; bottom: under SUI-5 PDP.

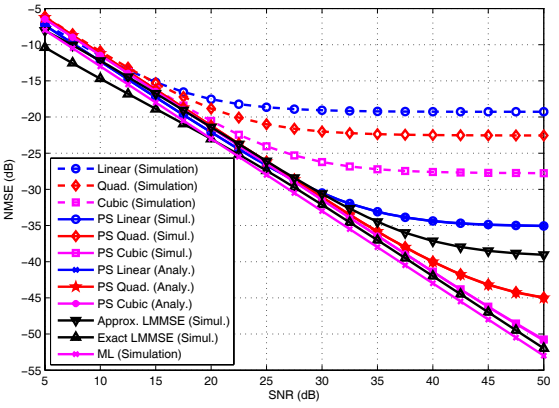

Fig. 4. NMSE of different channel estimation methods under the SUI-4 PDP with 25 samples of delay, where "PS" stands for "phase-shifted."

solution is quite poor in SUI-4 compared to phase-shifted polynomial interpolation, but is comparable to phase-shifted cubic interpolation in SUI-5 that has a longer delay spread. In a channel with reasonably short delay spread, such as SUI-4, phase-shifted cubic interpolation can provide comparable performance to exact LMMSE in medium to high SNR.

To verify that the proposed method is able to deal with inaccurate OFDM symbol timing, we simulate SUI-4 with 25

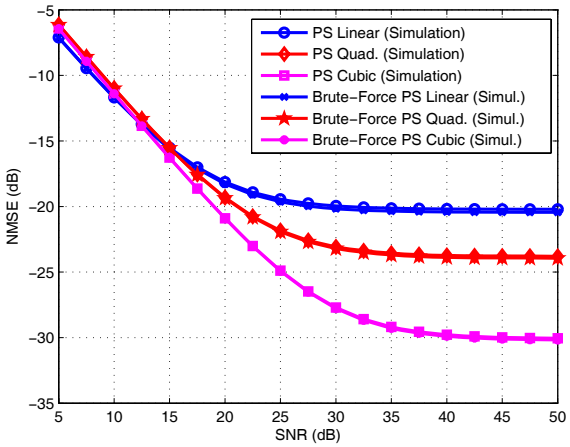

Fig. 5. Comparison of NMSE in channel estimation of the proposed method for finding the window shift with brute-force search at integer-sample granularity, where "PS" stands for "phase-shifted."

samples of initial delay. Fig. 4 shows the resultant performance of various channel estimators. Comparing with Fig. 3 (top plot), we see that the performance of the proposed method, as well as that of ML and exact LMMSE, stays unchanged. But conventional polynomial interpolation yields a much degraded performance due to the mechanism explained via Fig. 1. In contrast, the approximate LMMSE yields an improved performance, presumably because the 25 samples of initial delay makes the PDP closer to being uniform.

To see how much suboptimality the several approximations in Sections II-A and B may lead to, we compare the NMSE in channel estimation of the proposed method for finding the window shift to that achieved with brute-force search at integer-sample granularity. It turns out that the difference is very small. Fig. 5 shows the result for the SUI-5 channel.

IV. Performance Under the Mobile WiMAX Downlink Signal Structure

The Mobile WiMAX specifications furnish an interesting setting to test the performance of the proposed technique, especially since the number of pilots therein may be so few that ML interpolation cannot be applied to channels with moderate to long delay spreads.

The DL transmission of Mobile WiMAX is organized into "subframes." A subframe consists of an all-pilot OFDM preamble symbol followed by an even number of OFDM data symbols. The subcarriers in a data symbol are divided into "clusters" that contain 14 consecutive subcarriers each. A DL user signal consists of a number of subcarriers from a number of pseudo-randomly distributed (in frequency) clusters. The pattern of pilot subcarriers alternates in temporally successive OFDM symbols. Fig. 6 illustrates how pilots are placed in clusters. For convenience, in this section let $H(s,n)$ denote the channel response at the nth subcarrier of some cluster in symbol s. In a typical system with 10 MHz bandwith and $N = 1024$ [12], [13], there can be as few as 24 pilots in an OFDM symbol.

As the pilots are no longer of the comb type, the channel estimation method described earlier needs to be adjusted, and

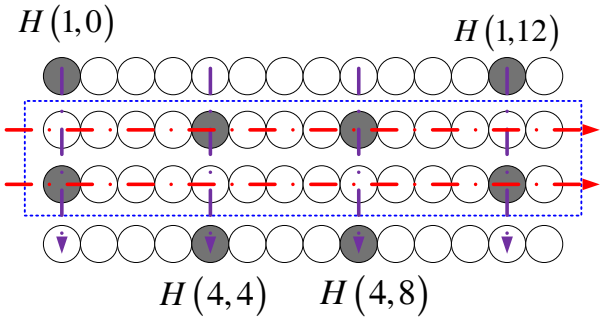

Fig. 6. Cluster structure in Mobile WiMAX downlink and corresponding channel estimation method. Each circle indicates a subcarrier and dark circles indicate pilot subcarriers. Four temporally consecutive clusters are shown, from top to bottom. The 14 subcarriers in a cluster are ordered from left to right.

so is the MSE analysis. Below we tailor the proposed channel estimation technique to suit the given DL signal structure and investigate the ensuing performance. We also propose a method to adaptively select the interpolation order for the best performance.

A. Channel Estimator Design

By the pseudo-random distribution of clusters, two "neighboring" clusters in a DL signal may not be adjacent in frequency. Thus it is simpler to perform channel estimation on clusters at different frequency positions separately than jointly. Now, in each cluster, there are only two pilot subcarriers whose distance varies with symbol index. In a typical system with 10 MHz bandwidth and $N = 1024$, two adjacent subcarriers are approximately 10 kHz apart. Hence in odd-numbered symbols the pilots are spaced by over 100 kHz, which is about the same order of magnitude as the coherence bandwidth of a typical urban outdoor channel [22]. Linear interpolation, even with optimal window shift, is not expected to yield good performance over this distance. In even-numbered symbols, extrapolation is needed for the many data subcarriers that lie outside the span of the pilots. Such extrapolation should be minimized because it amplifies the noise, for at least one extrapolation coefficient is greater than 1. Therefore, a good channel estimator should not limit itself to using the two only pilots in the current cluster, but should avail itself of the channel information at the two other pilot frequencies in temporally close clusters.

Concerning the window shift $\hat{\tau}$, since an integer value suffices for performance and can simplify the computation, we let $\hat{\tau}$ be an integer. In addition, to save computation, we estimate $\hat{\tau}$ only once per DL subframe from the preamble symbol employing the method of Section II-B. The resultant channel estimation method for the data symbols is as follows. For convenience, we describe it for the middle two (dash-boxed) symbols illustrated in Fig. 6 together.

1) Recall the value of $\hat{\tau}$ that has been estimated using the preamble symbol.
2) Circularly shift the signal samples in symbols 1 to 4 by $-\hat{\tau}$ samples before taking their DFT. This is equivalent to effecting a channel with phase-rotated frequency response $H_\tau(s,n) = e^{j2\pi\hat{\tau}f(n)/N}H(s,n)$ where $f(n)$ denotes the normalized frequency of subcarrier n. (We have used an adapted version of the notations in (7) here.)
3) Do LS channel estimation for pilot subcarriers in symbols 1 to 4. This yields, for each pilot with time-frequency index (s,n), a phase-rotated channel estimate $\hat{H}_\tau(s,n) = e^{j2\pi\hat{\tau}f(n)/N}\hat{H}(s,n)$. (We have used an adapted version of the notations in (8) here.)
4) Linearly interpolate in time to obtain $\hat{H}_\tau(2,0)$, $\hat{H}_\tau(2,12)$, $\hat{H}_\tau(3,4)$ and $\hat{H}_\tau(3,8)$.
5) Perform conventional Kth-order interpolation (and extrapolation) in frequency to obtain channel estimates for the remaining subcarriers in symbols 2 and 3. This corresponds to the operation described in (9), or equivalently, that in the last summation in (6).

Note that we do not have to carry out the phase-derotation indicated by the premultiplication with $e^{-j2\pi\tau(p+n)/N}$ in the RHS of (6), for by the circular signal shifting in step 2, the phase-rotated channel becomes what is needed for signal detection, not the phase-derotated. Note also that step 4 (temporal interpolation) results in four reference data points per cluster. Hence in step 5 we may employ an interpolation order up to three. To minimize the modeling error, in Kth-order interpolation of a data subcarrier's channel response the $K+1$ nearest pilots' responses are used. The performance of the proposed channel estimator is analyzed in Appendix B.

B. Simulation Examples

We simulate a system with carrier frequency = 2.5 GHz, bandwidth = 10 MHz, DFT size = 1024, and cyclic prefix length = 128. We let a DL subframe contain 24 OFDM symbols following the preamble. Again, we simulate the SUI-4 and SUI-5 PDPs with block-static fading at a rate corresponding to 100 km/h of mobile speed.

Fig. 7 shows some channel estimation performance results. (See curves marked by the first six legend items in each plot.) For SUI-4, the approximate analysis matches the simulation results almost exactly. For SUI-5, which has a larger delay spread than SUI-4, the approximate analysis is less accurate, but still follows the general behavior of the simulation results. The channel estimators show poorer performance under SUI-5 than under SUI-4, but the relative performance of the three interpolation orders are characteristically similar in both cases. In either channel, the MSE floors of lower-order interpolation start to manifest at lower SNR values than higher-order interpolation. As a rule, in higher pilot SNR, higher-order interpolators perform better by having lower frequency interpolation errors, but in lower pilot SNR, lower-order interpolators are better due to smaller AWGN effects.

C. Adaptive Selection of Interpolation Order

That the best interpolation order depends on the channel SNR suggests adaptive selection of the interpolator order. From the analysis in Appendix B, this can be accomplished if we can estimate σ_η^2, σ_t^2, and $\sigma_{\xi_K}^2(\tau^o)$ and use the results to predict the MSE via (44), (47), (48), and (49). The interpolation order that yields the least MSE can then be chosen.

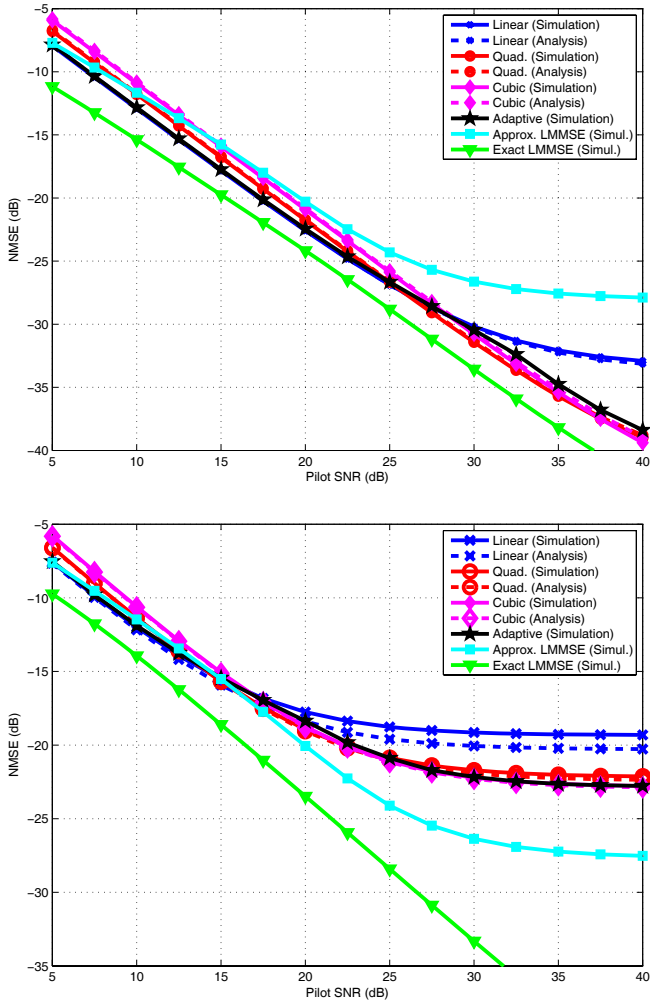

Fig. 7. NMSE of channel estimation in WiMAX DL transmission at 100 km/h mobile speed with fixed-order and adaptive interpolation. Top: over SUI-4 channel; bottom: over SUI-5 channel.

As the window shift $\hat{\tau}$ is determined once per DL subframe (see Section IV-A), the interpolation order is also determined once per DL subframe. As the quantity σ_t^2 (variance of temporal interpolation error) is a function of the time-variation of the channel, it is hard to estimate using only the preamble symbol. Thus we disregard it (and the center RHS term in (49)) in the selection of the interpolation order. For the other two quantities, σ_η^2 (variance of LS channel estimation error) can be relatively easily estimated using the null subcarriers in the preamble. As to $\sigma_{\xi K}^2(\tau^o)$, from (23) and (24) we can estimate it from the preamble symbol as

$$\hat{\sigma}_{\xi K}^2(\tau^o) = \frac{1}{F^{2K+2}}\left[P_K \hat{R}_0 + 2\min_{\tau} \gamma_K(\tau)\right] \tag{39}$$

where $\hat{R}_0 = \langle\langle |\hat{H}(f)|^2 \rangle\rangle - \hat{\sigma}_\eta^2$ with $\hat{\sigma}_\eta^2$ being an estimate of σ_η^2, and $P_1 = 6$, $P_2 = 20$, and $P_3 = 70$. In summary, for each DL subframe, we partially predict the MSEs for linear, quadratic, and cubic interpolations based on (49), with its center RHS term omitted, using the received preamble symbol. The interpolation order yielding the smallest predicted partial MSE is selected.

The performance of adaptive interpolation over the SUI-4 and SUI-5 channels is also illustrated in Fig. 7. We see that, by and large, the proposed scheme can choose the optimal interpolation order, though at times it may make an unfavorable decision. For comparison, the figure also shows the performance of 4-tap LMMSE estimation based on exact channel correlation (marked "exact LMMSE") and that based on a correlation function corresponding to uniform PDP of length equal to CP (marked "approx. LMMSE"). Again, the exact LMMSE has the best performance of all, but is unrealizable. On the other hand, the performance of the approximate LMMSE estimator is more erratic, because a uniform PDP may or may not be close to the characteristics of the instantaneous channel response at any given time.

V. Conclusion

We considered channel estimation by polynomial interpolation for multicarrier transmission. We showed that, by shifting the effective time window by a proper amount, the performance could be improved significantly. We derived a method to estimate the optimal window shift for arbitrary interpolation order. The method operates on frequency-domain quantities and is thus particularly suitable for pilot-aided multicarrier systems. It can be used where ML interpolation cannot for scarcity of pilots.

As a practical example, we considered the structure of Mobile WiMAX downlink signal and specialized the proposed technique for it. We also proposed a way to carry out adaptive selection of interpolation order based on some estimated MSE values. Simulation results showed that the adaptive scheme could yield nearly optimal performance over a wide range of SNR values. It may even compare favorably to LMMSE channel estimation.

Appendix A
Simplification of $\left[n^{K+1} - \mathbf{v}'_{nK}\mathbf{X}_{nK}^{-1}\mathbf{x}_{nK}\right]$

Let $\mathbf{z} = [z(x_{n0}), z(x_{n1}), \cdots, z(x_{nK})]'$ where $z(n) \triangleq n^{K+1} - \mathbf{v}'_{nK}\mathbf{X}_{nK}^{-1}\mathbf{x}_{nK}$. Then

$$\begin{aligned}\mathbf{z} &= \mathbf{x}_{nK} - [\mathbf{v}_{x_0 K}, \mathbf{v}_{x_1 K}, \cdots, \mathbf{v}_{x_K K}]' \mathbf{X}_{nK}^{-1}\mathbf{x}_{nK} \\ &= \mathbf{x}_{nK} - \mathbf{X}_{nK}\mathbf{X}_{nK}^{-1}\mathbf{x}_{nK} = \mathbf{0}.\end{aligned} \tag{40}$$

Thus x_{nk} is a root of $z(n)$ $\forall k \in \{0, \cdots, K\}$. Now that $z(n)$ is a $K+1$st-order polynomial in n by definition, we have

$$z(n) = C\prod_{k=0}^{K}(n - x_{nk}) \tag{41}$$

for some C. Further, since the n^{K+1} term in $z(n)$ has unity coefficient by definition, $C = 1$.

Appendix B
Performance Analysis for the Proposed WiMAX Channel Estimator

Four factors contribute to the channel estimation error. They are, in order of appearance in the algorithm steps, 1) suboptimality in the estimated window shift (introduced in step 1), 2) the AWGN (introduced in step 3), 3) modeling error due to temporal interpolation (introduced in step 4), and 4) modeling error due to frequency interpolation (introduced in step 5). Compared to the analysis in Section III, the only

additional factor is item 3. However, because of it the AWGN propagates among the subcarriers differently than in the earlier analysis. The temporal interpolation error itself propagates through step 5, too. Moreover, the pilots used for frequency interpolation in step 5 are chosen somewhat differently than in Section III and the bandedge subcarriers are no longer discarded. In short, we will need to redo some analysis. Again, item 1 is difficult to analyze but, fortunately, constitutes a minor contribution in the total MSE. Thus only the other three factors are analyzed. We assume that these three errors are uncorrelated.

First, consider the AWGN. It enters channel estimator computation through the LS channel estimation at the pilot subcarriers. Again, let σ_η^2 denote the noise variance of LS channel estimation at a pilot. This noise propagates to other subcarriers via step 4 (temporal interpolation) and step 5 (frequency interpolation). Via step 4, it contaminates $\hat{H}_\tau(s,n)$ where $(s,n) \in \{(2,0),(2,12),(3,4),(3,8)\}$. Since $\hat{H}_\tau(s,n) = [\hat{H}_\tau(s-1,n)+\hat{H}_\tau(s+1,n)]/2$, the noise variance in $\hat{H}_\tau(s,n)$ is given by

$$\sigma_{wK}^2(s,n) = \left(\frac{1}{2}\right)^2 \sigma_\eta^2 + \left(\frac{1}{2}\right)^2 \sigma_\eta^2 = \frac{1}{2}\sigma_\eta^2 \qquad (42)$$

for all K. Via step 5, it results in a noise variance

$$\sigma_{wK}^2(s,n) = \sum_{k=0}^{K} c_{nk}^2 \sigma_{wK}^2(s,x_{nk}) \qquad (43)$$

where $s \in \{2,3\}$, $n \in \{1,2,3,5,6,7,9,10,11,13\}$, and $x_{nk} \in \{0,4,8,12\}$, with c_{nk} indexed similarly to (3). Averaging over all data subcarriers, we obtain the average noise variance as

$$\sigma_{w1}^2 = 0.5130\sigma_\eta^2,\ \sigma_{w2}^2 = 0.6699\sigma_\eta^2,\ \sigma_{w3}^2 = 0.8121\sigma_\eta^2, \quad (44)$$

where the second subscript to σ gives the frequency interpolation order K as before (and similarly below).

Next, consider the modeling error in temporal interpolation. Its mean-square value is

$$\sigma_{tK}^2(s,n) = E\left|H_\tau(s,n) - \frac{1}{2}\left[H_\tau(s-1,n) + H_\tau(s+1,n)\right]\right|^2 \quad (45)$$

for $(s,n) \in \{(2,0),(2,12),(3,4),(3,8)\}$ for all K. With Rayleigh faded paths [15], [22],

$$\sigma_{tK}^2(s,n) = \sum_{l=0}^{L-1} A_l^2 \left[\frac{3}{2} - 2J_0(2\pi f_l) + \frac{1}{2}J_0(4\pi f_l)\right] \approx \frac{3\pi^4}{2}\sum_{l=0}^{L-1} f_l^4 A_l^2 \triangleq \sigma_t^2 \qquad (46)$$

where $A_l^2 = E|\alpha_l|^2$, f_l is the peak Doppler shift of path l times the OFDM symbol period, $J_0(\cdot)$ is the Bessel function of the first kind of order 0, and the approximation is obtained by expanding the Bessel function into a second-order Taylor series. Assume that the channel responses at different subcarriers are uncorrelated. Then a relation similar to (43) exists concerning the propagation of the temporal modeling error in the frequency domain via step 5. We get the average MSE as

$$\sigma_{t1}^2 = 0.4531\sigma_t^2,\ \sigma_{t2}^2 = 0.5577\sigma_t^2,\ \sigma_{t3}^2 = 0.6525\sigma_t^2. \quad (47)$$

Finally, consider the modeling error in frequency interpolation. The MSE at any data subcarrier is as given in (19), but the averages are different from that given in (31) due to the difference in choice of interpolating pilots as well as the presence of extrapolation for subcarrier 13. Straightforward numerical calculation yields the following average MSE:

$$\sigma_{e1}^2 = 2.6458\,\sigma_{\xi 1}^2(\tau^o),$$
$$\sigma_{e2}^2 = 12.8125\,\sigma_{\xi 2}^2(\tau^o),$$
$$\sigma_{e3}^2 = 93.0820\,\sigma_{\xi 3}^2(\tau^o). \qquad (48)$$

Put together, the overall average channel estimation MSE is given by

$$\sigma_K^2 = \sigma_{wK}^2 + \sigma_{tK}^2 + \sigma_{eK}^2. \qquad (49)$$

ACKNOWLEDGMENT

The authors would like to thank the reviewers whose comments helped improve the paper.

REFERENCES

[1] B. Yang, K. B. Letaief, R. S. Cheng, and Z. Cao, "Channel estimation for OFDM transmission in multipath fading channels based on parametric channel modeling," *IEEE Trans. Commun.*, vol. 49, pp. 467-478, Mar. 2001.

[2] M. Oziewicz, "On application of MUSIC algorithm to time delay estimation in OFDM channels," *IEEE Trans. Broadcasting*, vol. 51, no. 2, pp. 249-255, June 2005.

[3] O. Simeone, Y. Bar-Ness, and U. Spagnolini, "Pilot-based channel estimation for OFDM systems by tracking the delay-subspace," *IEEE Trans. Wireless Commun.*, vol. 3, no. 1, pp. 315-325, Jan. 2004.

[4] C.-J. Wu and D. W. Lin, "Sparse channel estimation for OFDM transmission based on representative subspace fitting," in *Proc. IEEE 61st Veh. Technol. Conf.*, 2005, vol. 1, pp. 495-499.

[5] O. Edfors, M. Sandell, J. J. van de Beek, S. K. Wilson, and P. O. Börjesson, "OFDM channel estimation by singular value decomposition," *IEEE Trans. Commun.*, vol. 46, no. 4, pp. 931-939, July 1998.

[6] Y. Li, "Pilot-symbol-aided channel estimation for OFDM in wireless systems," *IEEE Trans. Veh. Technol.*, vol. 49, no. 4, pp. 1207-1215, July 2000.

[7] M. Morelli and U. Mengali, "A comparison of pilot-aided channel estimation methods for OFDM systems," *IEEE Trans. Signal Process.*, vol. 49, no. 12, pp. 3065-3073, Dec. 2001.

[8] O. Edfors, M. Sandell, J. J. van de Beek, S. K. Wilson, and P. O. Börjesson, "Analysis of DFT-based channel estimators for OFDM," *Wireless Personal Commun.*, vol. 12, no. 1, pp. 55-70, Jan. 2000.

[9] Y. Li, L. J. Cimini, Jr., and N. R. Sollenberger, "Robust channel estimation for OFDM systems with rapid dispersive fading channels," *IEEE Trans. Commun.*, vol. 46, no. 7, pp. 902-915, July 1998.

[10] C. N. R. Athaudage and A. D. S. Jayalath, "Delay-spread estimation using cyclic-prefix in wireless OFDM systems," *IEE Proc.-Commun.*, vol. 151, no. 6, pp. 559-566, Dec. 2004.

[11] M.-H. Hsieh and C.-H. Wei, "Channel estimation for OFDM systems based on comb-type pilot arrangement in frequency selective fading channels," *IEEE Trans. Consumer Electron.*, vol. 44, no. 1, pp. 217-225, Feb. 1998.

[12] IEEE Stds. 802.16-2009, IEEE Standard for Local and Metropolitan Area Networks – Part 16: Air Interface for Fixed and Mobile Broadband Wireless Access Systems, IEEE, May 29, 2009.

[13] WiMAX Forum, Mobile WiMAX–Part I: A Technical Overview and Performance Evaluation, WiMAX Forum White Paper, Aug. 2006.

[14] J. Park *et al.*, "Performance analysis of channel estimation for OFDM systems with residual timing offset," *IEEE Trans. Wireless Commun.*, vol. 5, no. 7, pp. 1622-1625, July 2006.

[15] K.-C. Hung and D. W. Lin, "Optimal delay estimation for phase-rotated linearly interpolative channel estimation in OFDM and OFDMA systems," *IEEE Signal Process. Lett.*, vol. 15, pp. 349-352, 2008.

[16] R. W. Schafer and L. R. Rabiner, "A digital signal processing approach to interpolation," *Proc. IEEE*, vol. 61, no. 6, pp. 692-702, June 1973.

[17] K.-C. Hung and D. W. Lin, "Pilot-aided multicarrier wireless channel estimation via MMSE polynomial interpolation," in *IEEE Global Commun. Conf.*, Dec. 2008.

[18] S. Kay, "A fast and accurate single frequency estimator," *IEEE Trans. Acoust. Speech Signal Process.*, vol. 37, no. 12, pp. 1987-1990, Dec. 1989.
[19] E. K. Blum, *Numerical Analysis and Computation: Theory and Practice*. Reading, MA: Addison-Wesley, 1972.
[20] P. J. Davis and I. Polonsky, "Numerical integration, differentiation, and integration," in *Handbook of Mathematical Functions,* M. Abramowitz and I. A. Stegun, editors. Washington, DC: National Bureau of Standards, 1964, ch. 25, pp. 875-898.
[21] V. Erceg *et al.*, "Channel models for fixed wireless applications," Standards Contribution IEEE 802.16.3c-01/29r1, Feb. 23, 2001.
[22] T. S. Rappaport, *Wireless Communications Principles and Practice*, 2nd edition. Upper Saddle River, NJ: Prentice Hall, 2002.

Kun-Chien Hung received the B.S. and Ph.D. degrees in electronics engineering from the National Chiao Tung University, Hsinchu, Taiwan, R.O.C., in 2001 and 2008, respectively. He is currently a senior engineer with MediaTek Inc., Hisnchu. His research interests are in digital signal processing, communication receiver design, and wireless communication.

David W. Lin (S'79-M'81-SM'88) received the B.S. degree in electronics engineering from the National Chiao Tung University, Hsinchu, Taiwan, R.O.C., in 1975 and the M.S. and Ph.D. degrees in electrical engineering from the University of Southern California, Los Angeles, CA, U.S.A., in 1979 and 1981, respectively.

He was with Bell Laboratories during 1981-1983 and with Bellcore during 1984-1990 and again during 1993-1994. Since 1990, he has been a Professor with the Department of Electronics Engineering and Institute of Electronics, National Chiao Tung University, except for a leave in 1993-1994. He has conducted research in digital adaptive filtering and telephone echo cancellation, digital subscriber line and coaxial network transmission, speech and video coding, and wireless communication. His research interests include various topics in signal processing and communication engineering.